Materials Letters 270 (2020) 127697

Contents lists available at ScienceDirect

Materials Letters

journal homepage: www.elsevier.com/locate/mlblue

Stress-induced change of Cu-doped Bi_2Te_3 thin films for flexible thermoelectric applications

Byeong Geun Kim [a,1], Sang Hyun Bae [b,1], Jihyeon Byeon [a], Chun Lee [a], Soon-Mok Choi [b]

[a] Gyeongbuk Institute of IT Convergence Industry Technology, Research Development Division Vehicle Engineering Team, Gyeongsan-si 38463, South Korea
[b] School of Energy Materials Chemical Engineering, Korea University of Technology and Education, Cheonan-si 31253, South Korea

ARTICLE INFO

Article history:
Received 26 November 2019
Received in revised form 17 March 2020
Accepted 22 March 2020
Available online 25 March 2020

Keywords:
Thermoelectric
Bi_2Te_3
Sputtering
Substrates
Flexible
Polyimide

ABSTRACT

Cu-doped Bi_2Te_3 thin films were deposited on Si wafer, glass, and polyimide substrates at 200 °C using magnetron sputtering. During the deposition process, it is confirmed that thermal stress occurred at the films due to the mismatch of the coefficient of thermal expansion between the films and the substrates. As substrates with different coefficients of thermal expansion were used, the changes of crystal growth, morphologies, and thermoelectric properties of the Cu-doped Bi_2Te_3 thin films were investigated.

1. Introduction

Thermoelectric power serves to convert waste heat from our daily life or industrial sites into electricity, and has become a leading energy-conversion technology [1–3]. The importance of energy efficiency grows more critical day by day as the demand for energy-related products rapidly rises. Recently, IT devices have been developing at a very fast pace, and are gradually being miniaturized due to enhanced efficiency and for user convenience. Thermoelectric power can play a role in increasing the energy efficiency in various fields such as electric vehicles and portable and flexible IT devices. In particular, film-based thermoelectric devices are suitable for these applications due to the possibility of flexibility and thin shape [4]. However, little research on thermoelectric films or nanostructures has been reported in comparison with bulk thermoelectric materials.

The thermoelectric performance is estimated by a figure of merit (ZT), as follows: $ZT = \alpha^2 T\sigma/\kappa$, where α, T, σ, and κ are the Seebeck coefficient, absolute temperature, electrical conductivity, and thermal conductivity, respectively [1–3]. Control of the scattering of electrons and phonons in crystalline defects such as grain boundaries is hence important. Contrary to bulk materials, thin films essentially require substrates that support thin materials. This can induce thermal stress in films at high temperatures. As a result, unwanted secondary phases and/or new nanostructures are formed during the deposition process or after thermal treatment [5,6], which can significantly affect the thermoelectric properties of the films.

From a different point of view, we posited that crystalline engineering in films can be controlled by thermal stress. To verify this, we prepared Cu-doped Bi_2Te_3 (CBT) films with different substrates; Si, glass, and polyimide (PI). They were selected due to their different thermal expansion coefficients (CTEs), given as follows: Si (2.4×10^{-6} °C^{-1}), glass (3.18×10^{-6} °C^{-1}), and PI (16.61×10^{-6} °C^{-1}) [6–7]. The influence of thermal stress was investigated by comparing with the changes as a function of the substrates in this study.

2. Experimental procedure

CBT films were deposited by co-sputtering with Cu (99.999) and Bi_2Te_3 (99.999%) targets using a magnetron sputtering system. Cu and Bi_2Te_3 targets were put into radio frequency (RF) and direct current (DC) guns, and their applied powers were 8 W and 40 W, respectively. The base and working pressures were 5×10^{-5} Torr and 1×10^{-1} Torr, respectively. Ar gas (99.999%) was used with 100 sccm to produce Ar^+ plasma in the chamber. The deposition temperature was 200 °C, which was verified by a thermocouple inside the chamber. The deposition time was 30 min. Pieces of Si

[1] These authors contributed equally to this work.
E-mail address: smchoi@koreatech.ac.kr (S.-M. Choi)

https://doi.org/10.1016/j.matlet.2020.127697
0167-577X/

wafer, glass, and polyimide were used as substrates. CBT films with Si wafer, glass, and PI were denoted as CBT-Si, CBT-Glass, and CBT-PI, respectively. The morphology and the composition of the CBT films were analyzed using a field emission scanning electron microscope (FESEM) equipped with an energy-dispersive X-ray spectrometer (EDS). Using the cross-sectional observation with FESEM analyses, the average thickness of CBT-Si, CBT-Glass and CBT-PI was determined with 686.9 nm, 590.8 nm, and 619.6 nm, respectively. The compositions of the CBT films were determined as $Cu_{3.8}Bi_{41.8}Te_{54.4}$ (CBT-Si), $Cu_{4.3}Bi_{40.5}Te_{55.2}$ (CBT-Glass), and $Cu_{5.6}Bi_{40.2}Te_{54.2}$ (CBT-PI) by EDS mapping. The structural and electrical properties of the CBT films were determined by X-ray diffraction (XRD) and Hall measurement, respectively. The thermoelectric properties of the films were measured using a commercial device (RZ2000li, Ozawa Science Co.) under an Ar atmosphere at room temperature.

3. Results and discussion

XRD spectra of CBT-Si, CBT-Glass, and CBT-PI are shown in Fig. 1. All XRD peaks were indexed to Bi_2Te_3 phase (JCPDS no. 15-0863), and no secondary phases such as Cu, Cu_2Te, BiTe, and Bi_4Te_3 were observed. This means that poly-crystalline phases of Cu-doped Bi_2Te_3 were successfully formed. In the XRD spectrum of CBT-PI, the broad peak between 20 and 25° originated from PI substrates [8].

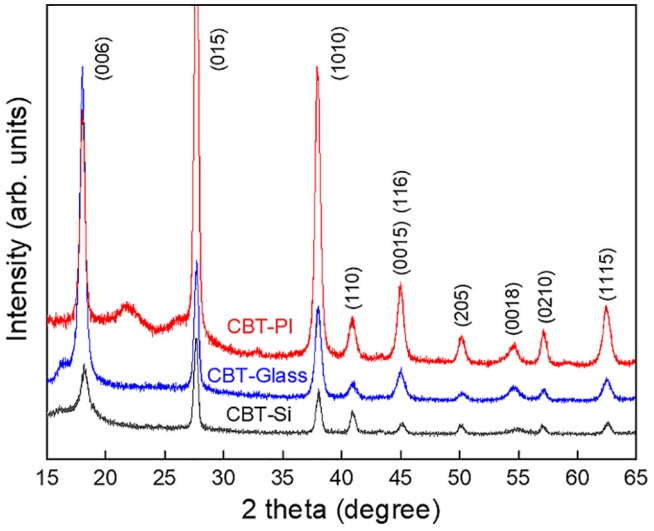

Fig. 1. XRD spectra of CBT films.

Fig. 2 presents thermoelectric properties of CBT films with different substrates at room temperature. Although they were deposited with the same deposition conditions, their characteristics differed greatly. CBT-Si had the highest electrical conductivity, followed by CBT-glass and CBT-PI (Fig. 2(a)): CBT-Si (1743.0 S/cm), CBT-Glass (1175.3 S/cm), and CBT-PI (930.1 S/cm). Seebeck coefficients of CBT-Si, CBT-Glass, and CBT-PI were 30.0 μV/K, 63.6 μV/K, and 84.6 μV/K, respectively (Fig. 2(b)). Although CBT-PI had the lowest electrical conductivity, its power factor was the highest at 665.4 $\mu W/K^2m$ because of its high Seebeck coefficient. CBT-Glass was followed by the lowest at 475.5 $\mu W/K^2m$, and CBT-Si was the lowest at 157.1 $\mu W/K^2m$. Comparing CBT-Si with CBT-PI, the gap of electrical conductivity between them was about twice as different. Hence, the values of the Seebeck coefficient and the power factor were about three-fold different (Fig. 2(a)). Considering that these films have been deposited under the same conditions, this is interesting. The first causes that can be inferred is the slight difference in Cu content as a function of the substrates. However, the Cu content of each film differs only by 1 to 2 at.% in this experiment. The thermoelectric properties of each film cannot be significantly different due to this small variation in doping contents [5,9]. Hence, we assumed that another factor is response for the change in the shape of the films.

Many crystals with hexagonal shape and layered structure were observed in the surface of CBT-Si (Fig. 3(a)). The number of the crystals protruding above the surface of film increased further in CBT-Glass (Fig. 3(b)), and CBT-PI (Fig. 3(c)) was completely composed of crystals. Moreover, the average size of the extruded crystals also depends on the substrates, the largest being in CBT-Si (477.8 nm), followed by CBT-Glass (410.3 nm) and CBT-PI (214.7 nm). This observation shows that the substrates have a significant effect on the growth behaviors and thermoelectric properties of the films, confirming that the main reason for the different electrical conductivities in the CBT films is the use of different substrates. Fig. 3(d)–(f) show that the cross-sectional features of CBT-Si, CBT-Glass and CBT-PI were significantly different each other. In CBT-Si and CBT-Glass, dense films were deposited with horizontal planes with the substrate, and some crystals protruded between them. Meanwhile, CBT-PI has columns of crystals stacked together resembling piled coins, and is very porous. The protruding crystals were assumed as 'hillocks', which is formed when strong

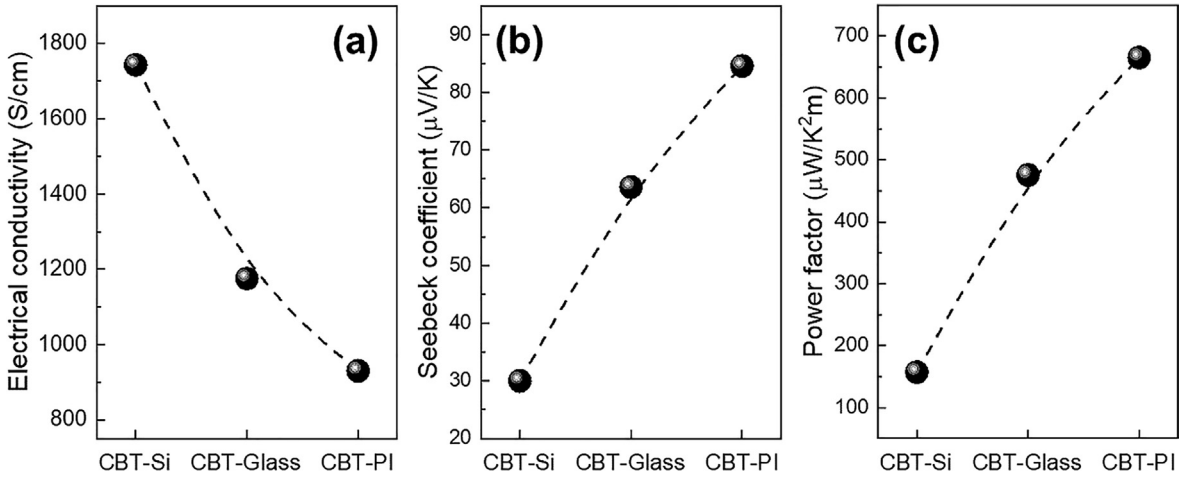

Fig. 2. Thermoelectric properties of CBT films: (a) electrical conductivities, (b) Seebeck coefficients, and (c) power factors.

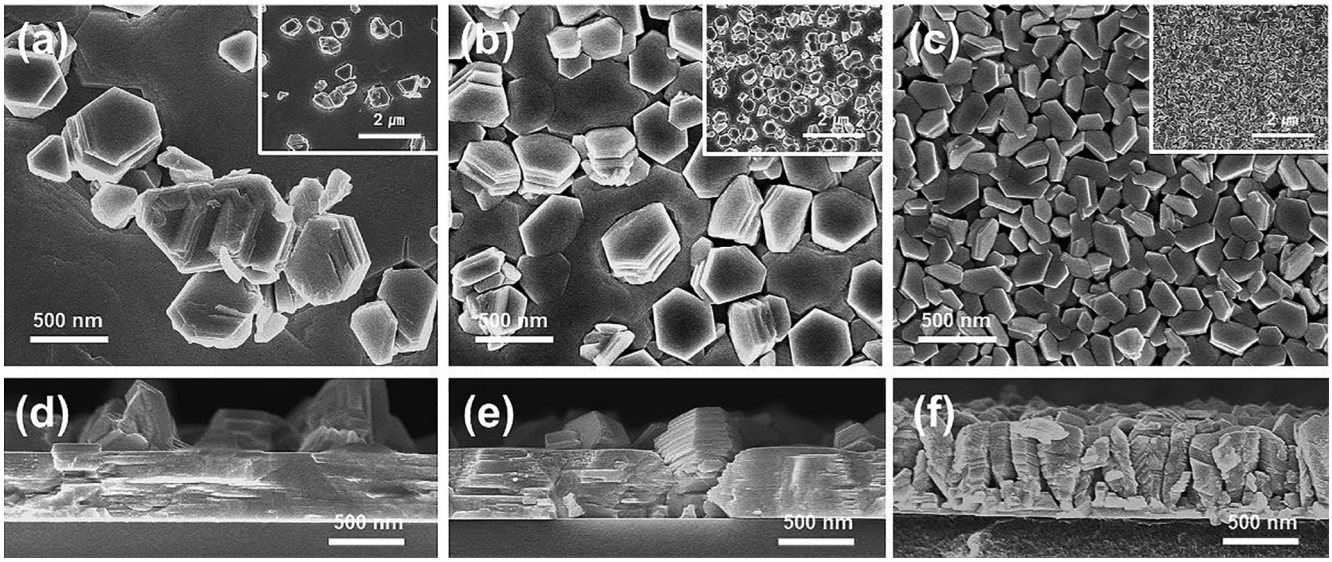

Fig. 3. Surface and cross-sectional FESEM images of (a) and (d) CBT-Si, (b) and (e) CBT-Glass, and (c) and (f) CBT-PI.

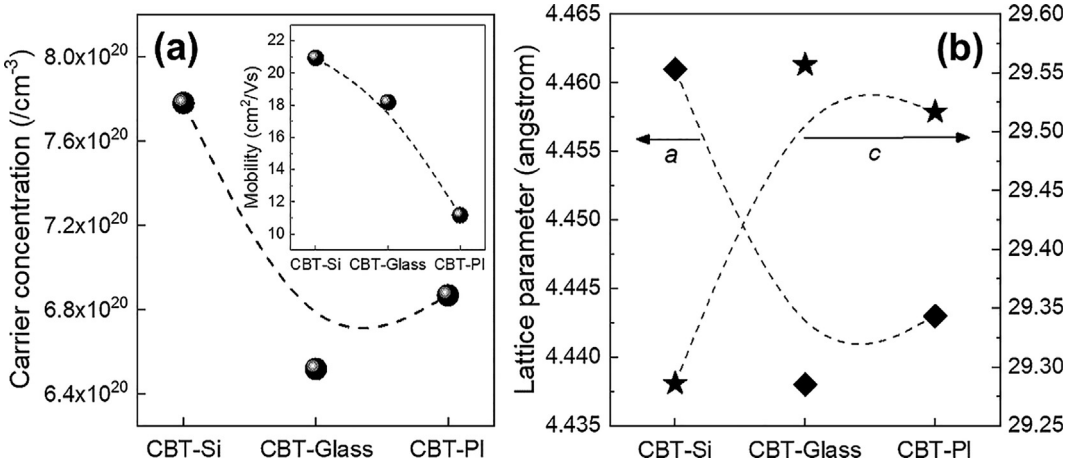

Fig. 4. (a) Electrical properties and (b) lattice parameters of CBT films.

compressive or tensile stress is applied to the growth of polycrystalline films [6,7,10]. This affects the shape and size of the crystals, and sometimes induces the formation of unexpected nanostructures such as nanowires [6,7].

Although no study on the CTE of CBT films has been reported, we suppose that it may be lower than that of the Si wafer because tensile stress occurred in CBT films. Based on the experimental results, the behaviors of thermal stress in different substrates are as follows: When the deposition process begins, substrates expand more than films because the CTE of CBT is smaller than that of Si, glass, and PI substrates, respectively. Tensile stresses are then generated in films due to the high values of CTE in substrates. The greater the difference in CTEs is, the greater the stress applied to the CBT films will be. Hence, the highest thermal stress occurs in CBT-PI, followed by CBT-Glass and CBT-Si.

The carrier concentration was the highest at CBT-Si, and the concentrations of the others were similar (Fig. 4). The carrier mobility of the CBT films was in the order of CBT-Si, CBT-Glass, and CBT-PI. The decrease of carrier mobility is due to the increase of new grain boundaries. First, the formation of hillocks provides new crystalline defects for electrons to scatter: the higher the number of hillocks is, the lower the electrical conductivity will be (Fig. 2). Second, CBT-PI has the smallest crystal size and a column structure wherein carriers can be highly scattered. As a result, it had the lowest mobility of carriers. In our study, CBT-PI has the highest power factor and porous morphology. In addition, the lattice parameters of CBT films were calculated from the XRD results (Fig. 4(b)): the *c*-axis lattice parameters of CBT-Glass and CBT-PI were larger than the CBT-Si case. This is ascribed to the Cu-intercalation into the gap of van der Waals between $Te^{(1)}$ and $Te^{(1)}$. The Cu-intercalation may act as a donor, which was confirmed by the lower carrier concentration of these systems than the CBT-Si cases (Fig. 4(a)). For the CBT-Si case, in turn, the Cu may be substituted for the Bi site. The substitution can increase the *p*-type carrier concentration.

4. Conclusions

CBT-Si, CBT-Glass, and CBT-PI were prepared to investigate the influence of substrates. No secondary phases were found in the XRD spectra in the CBT films, and Bi_2Te_3 phases were detected. Many hillocks were observed in CBT-Si, and their number gradually increased in CBT-Glass and CBT-PI. The average size of the hillocks was highest and lowest in CBT-Si and CBT-PI, respectively. This observation is evidence of the occurrence of tensile stress in films. The highest and lowest stresses occurred in CBT-PI and

CBT-SI, respectively. Although the electrical conductivity of CBT-PI was the lowest, its power factor was the highest.

CRediT authorship contribution statement

Byeong Geun Kim: Conceptualization, Writing - original draft, Investigation, Writing - review & editing, Funding acquisition. **Sang Hyun Bae:** Writing - original draft, Investigation, Formal analysis. **Jihyeon Byeon:** Formal analysis. **Chun Lee:** Formal analysis. **Soon-Mok Choi:** Conceptualization, Writing - original draft, Writing - review & editing, Supervision, Funding acquisition.

Declaration of Competing Interest

The authors declare that they have no known competing financial interests or personal relationships that could have appeared to influence the work reported in this paper.

Acknowledgments

This research was supported by the Basic Science Research Program (NRF-2017R1D1A1A09000570) and by a grant from the Industrial Core Technology Development Program (10083640). And thanks the Cooperative Equipment Center at KOREATECH for assistance with SEM XRD analysis. This research was also supported by Basic Science Research Program through the National Research Foundation of Korea (NRF) funded by the Ministry of Education (2018R1D1A1A02086218).

References

[1] G.J. Snyder, E.S. Toberer, Nat. Mater. 7 (2008) 105–114.
[2] S.I. Kim, K.H. Lee, H.A. Mun, H.S. Kim, S.W. Hwang, J.W. Roh, D.J. Yang, W.H. Shin, X.S. Li, Y.H. Lee, G.J. Snyder, S.W. Kim, Science 348 (2015) 109–114.
[3] R. Venkatasubramanian, E. Siivola, T. Colpitts, B. O'Quinn, Nature 413 (2001) 597–602.
[4] S.J. Kim, J.H. We, B.J. Cho, Energy Environ. Sci. 7 (2014) 1959–1965.
[5] K.H. Seo, B.G. Kim, C.-H. Lim, S.-H. Kim, K.-M. Lee, J.-Y. Kim, S.-M. Choi, CrystEngComm 19 (2017) 2750–2757.
[6] B.G. Kim, B.-S. Kim, S.-M. Jeong, S.-M. Choi, D. Whang, H.-L. Lee, S.-H. Hyun, CrystEngComm 14 (2012) 4255–4258.
[7] J. Ham, W. Shim, D.H. Kim, S. Lee, J. Roh, S.W. Sohn, K.H. Oh, P.W. Voorhees, W. Lee, Nano Lett. 9 (2009) 2867–2872.
[8] B.G. Kim, S.-M. Choi, C.-H. Lim, J. Nanosci. Nanotechnol. 17 (2017) 7677–7680.
[9] F.R. Sie, C.H. Kuo, C.S. Hwang, Y.W. Chou, C.H. Yeh, Y.L. Lin, J.Y. Huang, J. Electron. Mater. 45 (2016) 1927–1934.
[10] Y. Yue, M. Chen, Y. Ju, L. Zhang, Scr. Mater. 66 (2012) 81–84.